

**PRACTICAL SUPERCONDUCTOR DEVELOPMENT
FOR ELECTRICAL POWER APPLICATIONS
ARGONNE NATIONAL LABORATORY
QUARTERLY REPORT FOR THE PERIOD ENDING JUNE 30, 2004**

This is a multiyear experimental research program that focuses on improving relevant material properties of high-critical-temperature (T_c) superconductors and developing fabrication methods that can be transferred to industry for production of commercial conductors. The development of teaming relationships through agreements with industrial partners is a key element of the Argonne National Laboratory (ANL) program.

Technical Highlights

Several findings are highlighted. We continued investigating the effect of substrate inclination angle α on the properties of $\text{YBa}_2\text{Cu}_3\text{O}_{7-x}$ (YBCO)-coated conductors made by the Inclined Substrate Deposition (ISD) method. As α increased, the tilt of YBCO (00 l) planes increased relative to the substrate surface. YBCO films deposited on substrates with $\alpha = 35$ and 55° had the best in-plane texture (giving FWHM values of 6.54 and 6.20° , respectively) and the highest J_c values. We describe Raman microscopy analyses of a 12-meter long YBCO coated conductor produced by SuperPower, Inc. and correlate the results with centimeter-by-centimeter I_c measurements made at SuperPower. We also provide an update on efforts to design a Raman probe suitable for on-line examination of YBCO films on coated conductor tape.

YBCO Films on SrRuO_3 (SRO)-Buffered ISD-MgO Substrates

Samples that are presently made by the ISD method have the architecture YBCO/SRO/HE-MgO/ISD-MgO/YSZ/HC, in which a single SrRuO_3 (SRO) buffer layer replaces the CeO_2 and uppermost YSZ layer of ANL's original ISD architecture [1]. Samples with the present-day architecture will be represented in the remainder of the report by the shorthand notation YBCO/SRO/ISD. In this structure, the ISD-MgO layer is deposited by electron beam evaporation (EBE) with the substrate at an inclination (α) whose value affects important characteristics of the ISD-MgO layer, e.g., the tilt of its surface relative to the substrate surface (β), its surface roughness, and its in-plane texture [2]. Until recently, the value of α was set at 55° during deposition of all ISD-MgO layers, because it appeared to give films with the sharpest texture and lowest surface

roughness. We showed last quarter, however, that ISD-MgO films made with $\alpha = 35^\circ$ consistently have higher transport J_c despite their slightly poorer in-plane texture and larger roughness. Because this finding suggested that the tilt of ISD-YBCO films influences their superconducting properties, we studied the superconducting and crystalline properties of conductors made with $\alpha = 15, 20, 25, 30, 35, 40, 45, 50,$ and 55° .

Small ($1.0 \times 0.5 \times 1.2 \text{ cm}^3$) coupons of Hastelloy C (HC), polished to a mirror-finish by SuperPower, were mounted on a tiltable substrate stage using silver paste, and then YSZ (thickness, 300 \AA) was deposited on them by electron beam evaporation (EBE). Next, an ISD-MgO layer (thickness, 1 \mu m) was deposited on the YSZ at a deposition rate of 20 \AA/s using EBE at room temperature with α in the range of $15\text{-}55^\circ$. On top of the ISD-MgO layer was deposited an HE-MgO layer (thickness, 0.25 \mu m) using EBE with $\alpha = 0^\circ$ at 700°C .

The ISD substrates were then attached to a heated stage using silver paste, and SRO and YBCO films were deposited by pulsed laser deposition (PLD). A KrF excimer laser (Lambda Physik, Compex 201) with pulse duration of 25 ns and wavelength of 248 nm was focused onto the targets, which were rotated at 8 rpm . The YBCO and SRO targets (from Praxair Surface Technology) were 99.9% pure and had a diameter of 2.54 cm and a thickness of 0.63 cm . The distance between the substrate and target was 6.5 cm . The SRO film was deposited at 770°C for 20 min in 50 mtorr of O_2 using a laser energy of 128 mJ/pulse and frequency of 4 Hz . YBCO was deposited onto the SRO layer at 770°C in 240 mtorr of O_2 (deposition time, 30 min) using laser energy of 140 mJ/pulse and frequency of 8 Hz . After deposition, the YBCO films were annealed for 90 min inside the PLD chamber at 450°C in 1 atm O_2 .

Figure 1 shows the tilt angle β of YBCO (005) planes as a function of α . Last quarter we showed the effect of the inclination angle α on the tilt angle β of the ISD MgO template layer. The value of β was estimated from the strongest pole of the YBCO pole figure [2], and was found to increase as α increased. Comparing YBCO films on substrates with $\alpha = 35$ and 55° , β was $\approx 10^\circ$ smaller for films made with $\alpha = 35^\circ$.

Figure 2 indicates the effect of α on the transport and crystallographic properties of YBCO films deposited on ISD substrates with α in the range $15\text{-}55^\circ$. In-plane texture was evaluated using full width at half-maximum (FWHM) values of YBCO (005) scans. J_c was measured by the four-probe method. YBCO showed no in-plane texture and had a negligible J_c when it was deposited on a substrate made at $\alpha = 15^\circ$. YBCO films deposited on substrates with $\alpha = 35$ and

55° had good in-plane texture, giving the smallest FWHM values (6.54 and 6.20°, respectively) and the highest J_c values. The highest J_c value (1.2 MA/cm²) was observed for a film with $\alpha = 35^\circ$, and the second highest value (0.49 MA/cm²) was observed for a film with $\alpha = 55^\circ$. Films made on substrates with $35 < \alpha < 55^\circ$ had larger FWHM values, but the values were only slightly larger ($\approx 8^\circ$) in some cases; J_c values were correspondingly smaller, although some films had $J_c > 0.4$ MA/cm². Films on substrates with $\alpha < 35^\circ$ had the largest FWHM values ($\geq 10^\circ$), and their J_c values were the lowest, typically ≤ 0.1 MA/cm².

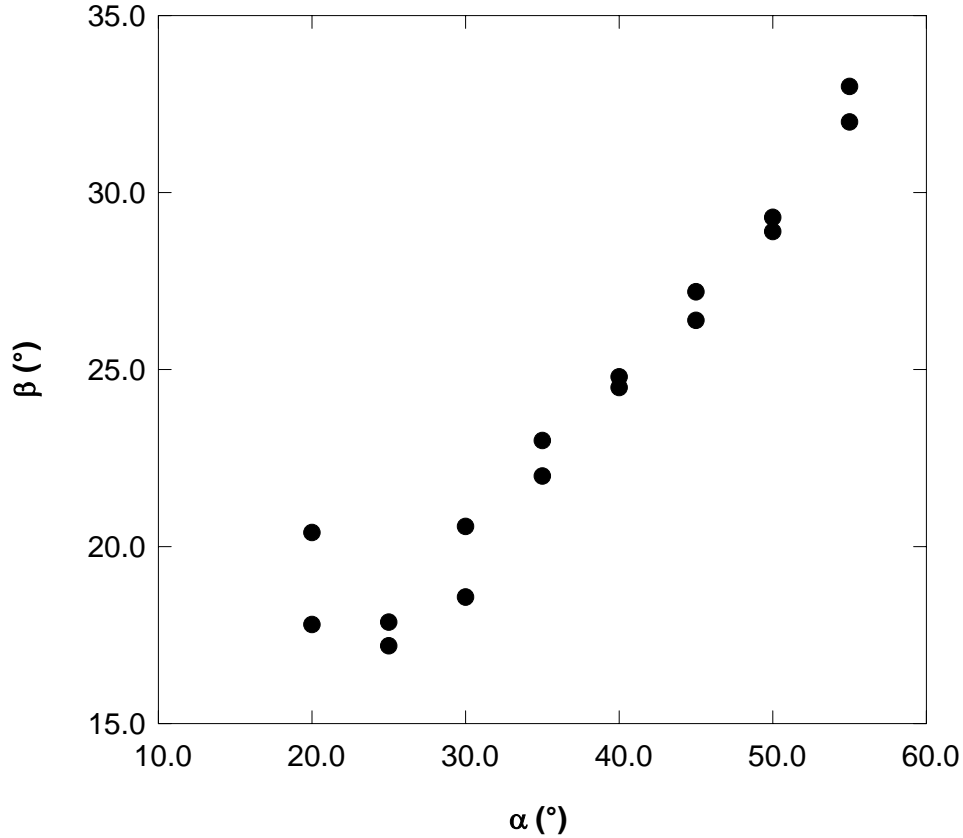


Fig. 1: Tilt angle β as function of α for YBCO (005) plane on YBCO/SRO/ISD-MgO substrate.

The superconducting transition temperature T_c and transition width ΔT of the YBCO films were measured using an inductive magnetization method. Figure 3 shows T_c and ΔT as a function of α . YBCO films deposited on substrates with $\alpha > 15^\circ$ all had $T_c > 87$ K and $\Delta T \approx 2$ K or less. Films with high transport J_c values had significantly sharper transitions, with $\Delta T < 1$ K. The film deposited

on a substrate with $\alpha = 15^\circ$, however, exhibited no T_c above 77 K.

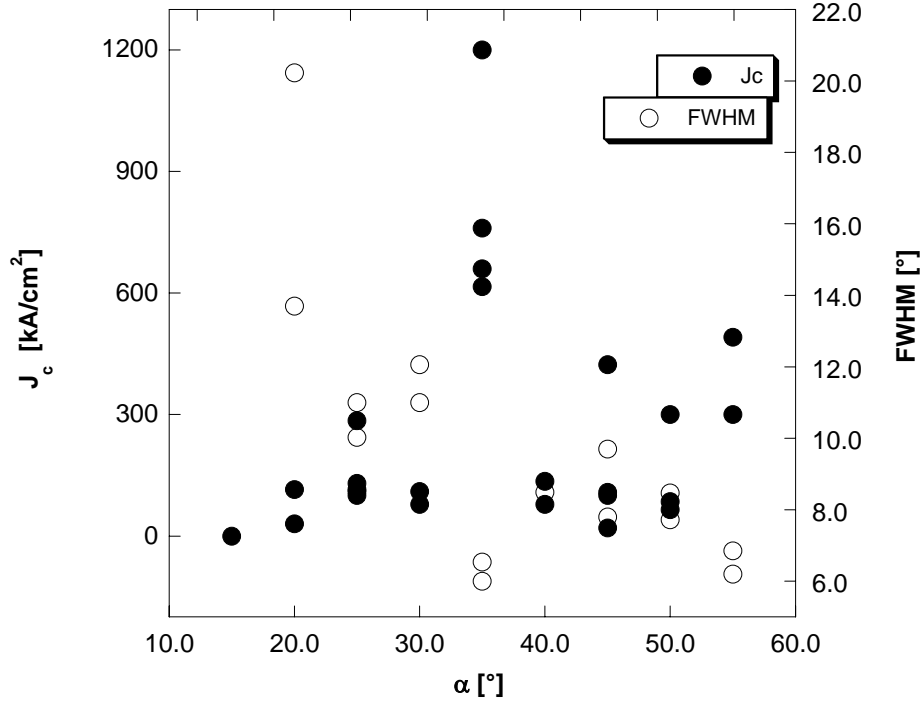


Fig. 2: Transport J_c and x-ray ϕ -scan FWHM values for YBCO (005) peak as function of substrate inclination angle α .

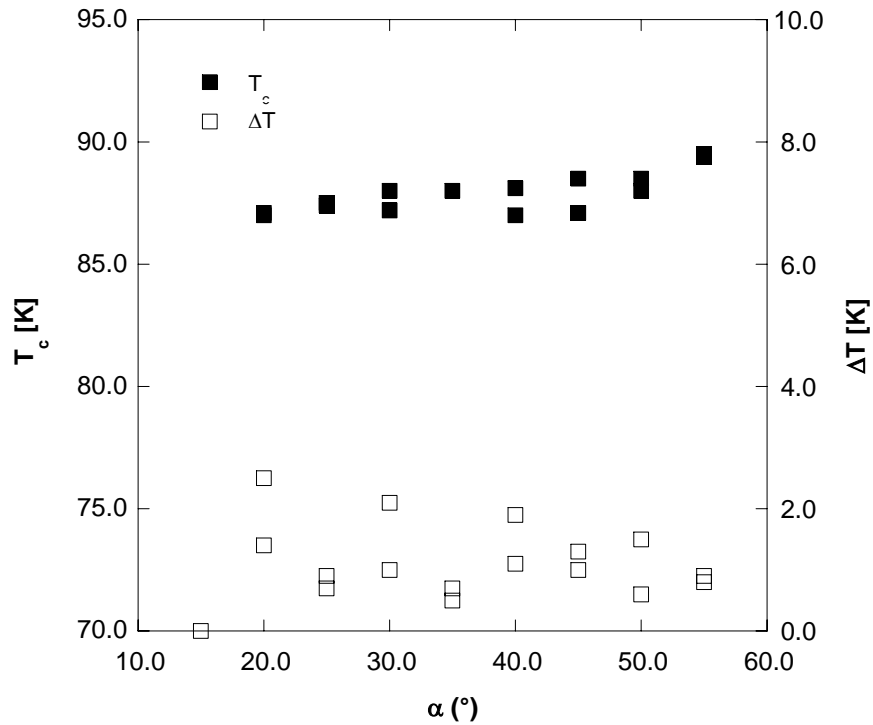


Fig. 3: Inductive T_c and superconducting transition temperature width ΔT as function of α for YBCO films grown on SRO buffered ISD-

MgO substrate.

Raman Study of 12-Meter Coated Conductor Produced by SuperPower, Inc.

At ANL, we are in the process of performing detailed characterization studies of long-length YBCO coated conductor (CC) specimens produced by SuperPower, Inc. Part of the characterization protocol includes Raman microscopy analysis of the YBCO film on segments of fully processed tape for which incremental critical current (I_c) measurements have also been made. The reel-to-reel (R2R) Raman microscopy measurement technique and data interpretation guidelines used in this work have been reported in previous Quarterly Reports and in a recent publication [3]. In this report we describe the results of analyses of a 12-meter long MOCVD CC tape. The YBCO film ($\approx 1 \mu\text{m}$ thick) was deposited on a CeO_2/IBAD -template/ Ni -alloy substrate. Centimeter-by-centimeter I_c measurements made at SuperPower revealed regions of relatively high and relatively low I_c as indicated in Fig. 4. Note in Fig. 4 that these regions of high and low I_c can occur in close proximity to one another.

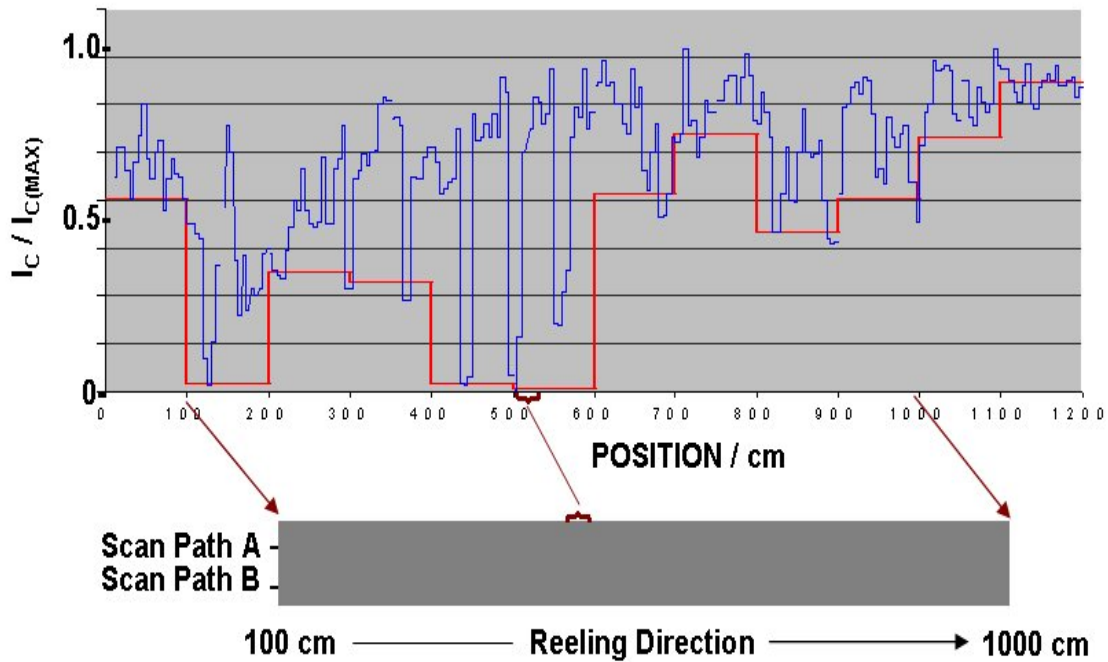


Fig. 4: Plot of normalized I_c ($I_c/I_{c(\text{MAX})}$) versus position along 12-m MOCVD YBCO CC tape produced by SuperPower, Inc. Sketch below graph identifies segment of tape probed by Raman microscopy and shows general location of scan paths tracked during Raman survey.

To perform the Raman examinations of this 12-m tape, the silver cap layer was removed from selected 15-20 cm segments along the length of the tape exposing the YBCO film surface. Raman scans of each exposed segment were made in centimeter increments along each of the two “scan paths” indicated in Fig. 4 to provide composition information in both the rolling and transverse directions. Representative Raman spectra from selected spots along the length of the tape are displayed in Fig. 5. (The numbers along the right edge indicate the centimeter position with respect to the horizontal axis in Fig. 4.)

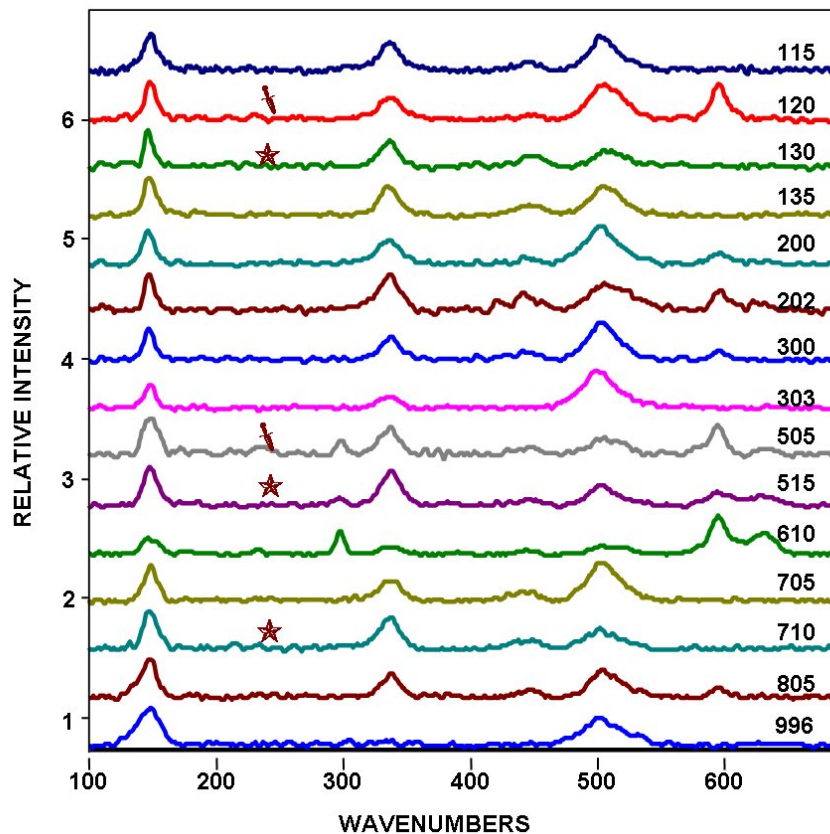


Fig. 5. Raman spectra from selected locations between 100 cm and 1000 cm marks in Fig. 4. Numbers on right of plot correspond to position (in cm) in Fig. 4.

The spectra in Fig. 5 reveal a clearly discernible variability in YBCO film composition along the length of the tape. The modes at ≈ 150 , 320 , and 500 cm^{-1} are the Cu_2 , $\text{O}_2^+/\text{O}_3^-$, and O_4 modes of YBCO [3]. As we have pointed out in previous reports (see, e.g., [3]), the appearance of the O_4 mode with comparable intensity to the $\text{O}_2^+/\text{O}_3^-$ mode in the measurement geometry of our R2R Raman microprobe scans generally informs that there is an appreciable amount of tilted

c-axis YBCO grain structure. Note in Fig. 5 that this condition is prevalent in a majority of the presented spectra. The mode at $\approx 300 \text{ cm}^{-1}$ is from CuO, while the modes in the $600 \pm 20 \text{ cm}^{-1}$ region are due to varying combinations of barium cuprate phases and cation disorder in the YBCO phase [3]. The spectral differences between relatively high I_c locations (indicated by a star in Fig. 5) and relatively low I_c locations (indicated by a dagger in Fig. 5) are noteworthy in that there tends to be less of the YBCO O4 mode and/or less of the nonsuperconducting second phase modes in the high I_c segments.

Selected segments were probed in closer detail by obtaining Raman scans in fraction-of-a-centimeter increments across the entire segment. A typical result of this more detailed type of interrogation is shown in Fig. 6 for the segment between 500 and 515 cm in Fig. 4. (The basis and methodology for producing the type of contour plot in Fig. 6a has been described in [3].) Here in Fig. 6a we see that the 500-503 cm portion is dominated by the O4 mode and the 503-510 cm portion contains an appreciable amount of barium cuprate phases plus some evidence of oxygen disorder in the YBCO, while the 510-515 cm portion is characterized by reduced barium cuprate presence and diminishing YBCO O4 mode intensity (relative to YBCO O2+/O3- intensity) along with narrowing of the Cu2 and O2+/O3- modes. The relative I_c values in this same segment of tape are shown in Fig. 6b for comparison purposes. Not surprisingly, the portion with the least second phase and the least evidence of c-axis tilt has the highest I_c .

Assistance to SuperPower in Qualifying, Procuring, and Implementing an On-Line Raman Probe

Over the past year we have continued to work on the conceptual design of a Raman probe suitable for on-line examination of the YBCO film on coated conductor tape. The design concept that we have arrived at is diagrammed in Fig. 7. This instrument setup provides the capability to examine moving tape, vary and maintain laser focus (spot size), and actually view the tape surface. A fiber optic cable brings the laser beam to the fiber optic head that sends a collimated beam to the focusing lens at the tip of the beam conduit. Raman scattering from the film surface is collected by the same lens, collimated, and sent back to the fiber optic head, which directs it through a second fiber optic cable to the monochromator. The beam pickoff optic directs a small fraction of the collimated scattered light to a photodiode that drives a focus control servo system. Also, the same pickoff optic can be used to direct white light to the sample surface and return optical images of the surface to a camera. (Raman measurement and optical viewing can be done sequentially but not

simultaneously.) Kaiser Optical Systems, Inc. (KOSI) markets a Raman system that provides much of the capability illustrated in Fig. 7.

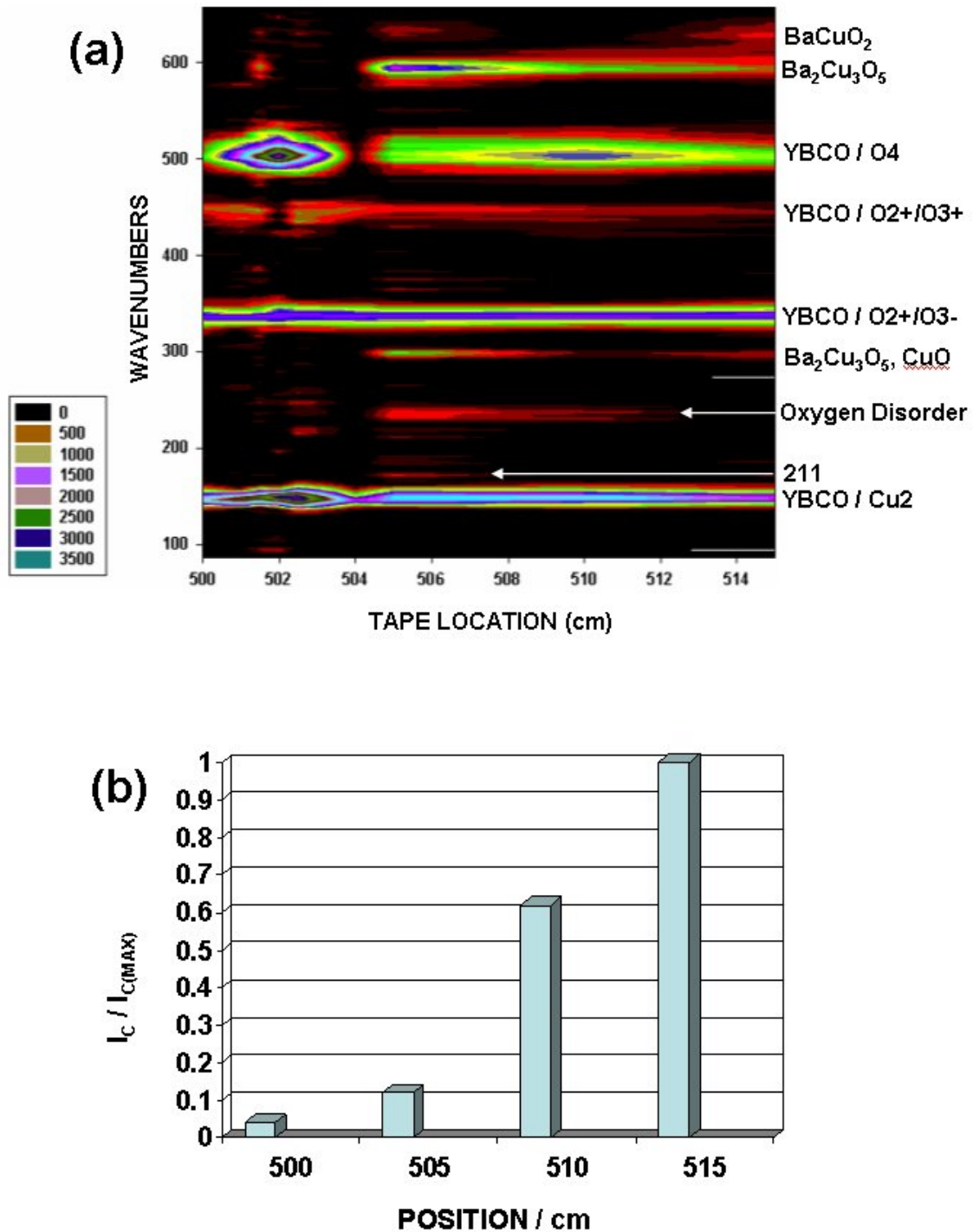


Fig. 6. (a) Intensity relief graphic constructed from closely spaced Raman scans recorded between 500 and 515 cm positions in Fig. 4. (All phonon intensities are normalized to intensity of YBCO O2+/O3-

mode at $\approx 320 \text{ cm}^{-1}$.) (b) Graph showing normalized I_c at four positions between 500 and 515 cm^{-1} .

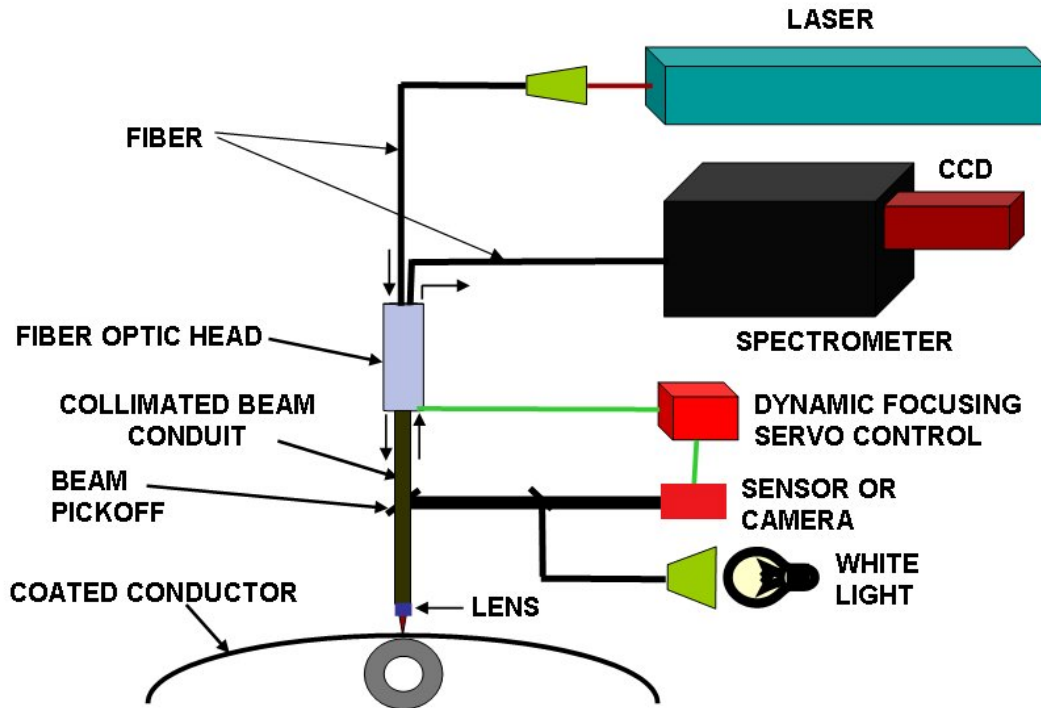


Fig. 7. Schematic diagram of Raman probe concept devised for on-line monitoring of moving CC tape after YBCO deposition.

During the past two quarters of FY 2004, V. Maroni made two trips to KOSI's plant to conduct proof-of-concept tests; J. Reeves of SuperPower, Inc. accompanied him on one of these trips. After these visits to KOSI, SuperPower purchased a Raman probe system from KOSI, and Maroni and Reeves performed more testing of the system at SuperPower's facility in Schenectady, NY.

A wide range of working parameters was investigated during the tests at KOSI and at SuperPower, including focusing effects, excitation laser wavelength (λ) and spot size, spatial variability of the Raman spectra in typical tape specimens, and development of a standard spectra database. These tests provided many useful insights about the functional aspects of the Raman probe approach:

(1) Maintaining optimum signal-to-noise conditions requires keeping the excitation laser in focus on the tape surface. The photon count levels for the Raman bands drop off rapidly as the beam moves out of focus.

(2) Typically, for YBCO films on buffered metal substrates, the character of the observed Raman spectrum is strongly dependent on the excitation laser spot size. Small (1-2 μm) spot sizes tend to give spectra of whatever crystalline phase the laser is striking. As the spot size is increased, the laser tends to cover more of the specimen area and adjacent phases are also detected. This effect is illustrated in Fig. 8 where we show spectra taken at one location in a low- I_c region and at another location in a high- I_c region of a 50-m MOCVD tape obtained from SuperPower. The Raman microprobe at Argonne ($\lambda = 633 \text{ nm}$) was used to collect these spectra, but no attempt was made to select a specific spot on the surface using the microscope. Instead, the laser was focused at an arbitrarily chosen spot. The bottom spectrum (taken in the low- I_c region) was obtained with a 2 μm spot size, then, without moving the specimen, the laser spot size was increased to 8 μm , and the next spectrum up was recorded. The interpretation of the bottom two spectra (Fig. 8) is that the laser strikes primarily a CuO crystallite at the 2 μm spot size, whereas it covers mostly YBCO at the 8 μm spot size. The top two spectra, taken at an arbitrarily selected location in a high- I_c region, are much the same for both the 2 and 8 μm spot sizes, which indicates the type of uniformity that we would hope/expect to see for high performance YBCO films on long-length coated conductors.

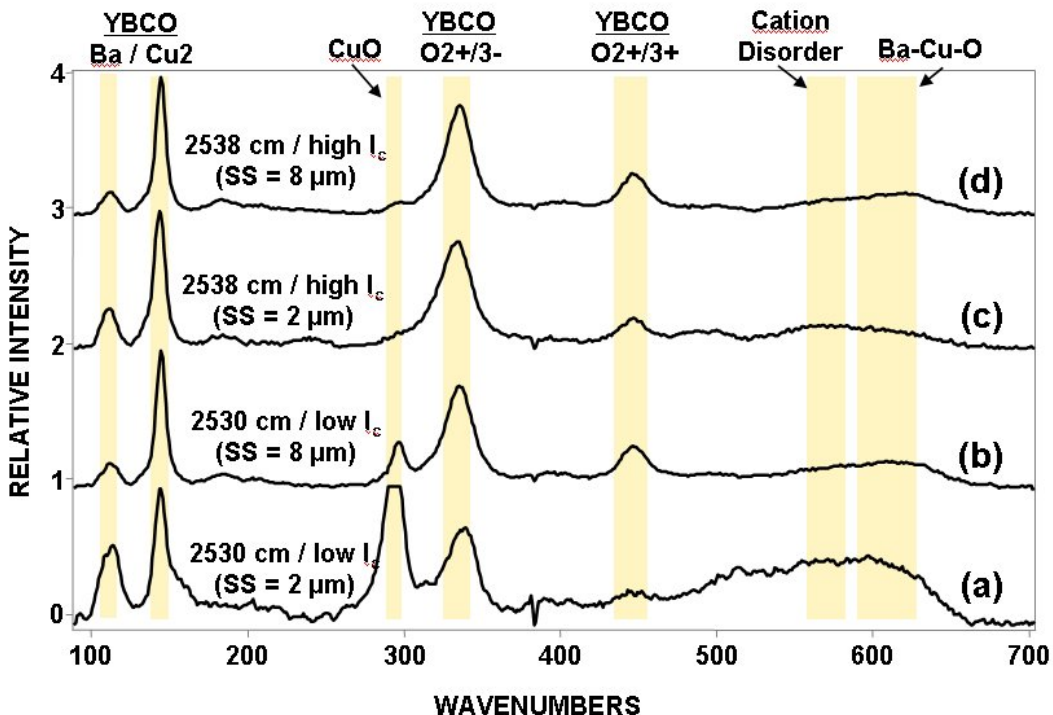


Fig. 8. Raman spectra recorded as function of laser spot size (SS) at two arbitrarily chosen positions on 50-m MOCVD YBCO CC tape produced by SuperPower, Inc. Spectra (a) and (b) were from low- I_c region; spectra (c) and (d) were from a high- I_c region.

(3) The results in Fig. 9 illustrate the composition uniformity issue in a different way. Here we show in the bottom and middle spectra the type of spectral change that can occur when we arbitrarily move an 8 μm laser spot 2 mm on a given specimen (in this case a low- I_c region of the SuperPower 50-m tape). Again, as we move from “Spot 1” to “Spot 1 + 2mm”, we appear to move further off of a CuO crystallite and on to more YBCO. Also shown in Fig. 9 (top spectrum) is how laser wavelength affects the relative intensities of YBCO and second phase phonons. The top spectrum in Fig. 9 was taken at a location near where the middle and bottom spectra were taken, but using the KOSI ($\lambda = 785$ nm) instrument instead of the Argonne ($\lambda = 633$ nm) instrument. We are still in the process of sorting out these λ -dependent intensity differences, so that we can better correlate results obtained at Argonne with results that are now being obtained at SuperPower.

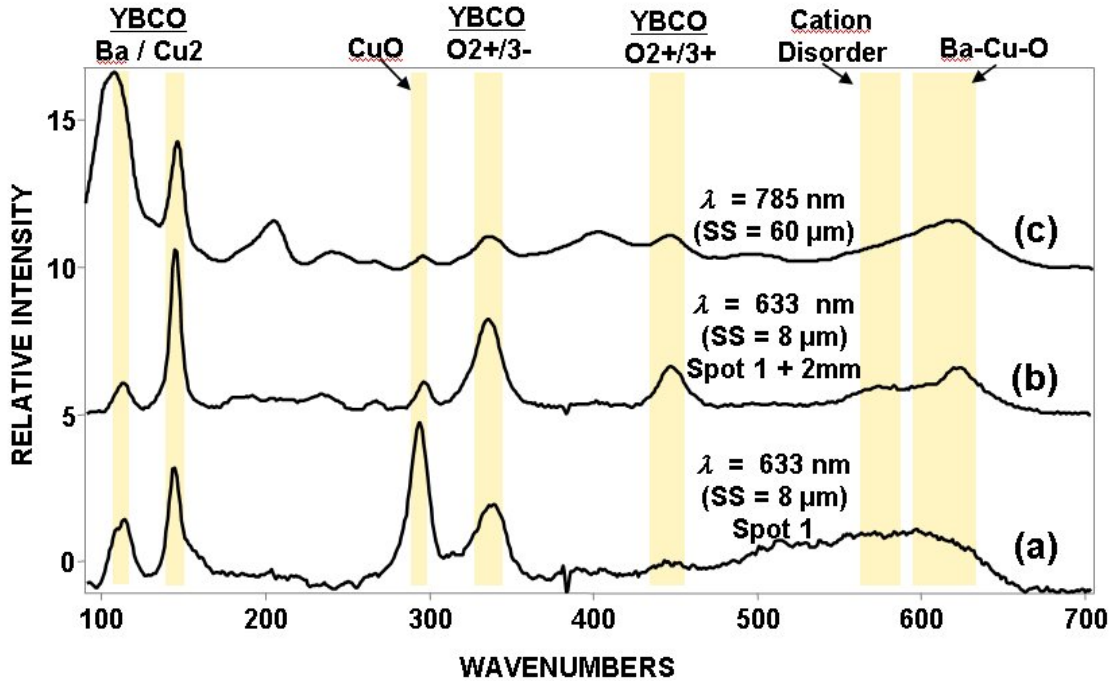


Fig. 9. Raman spectra recorded versus proximal location and laser excitation wavelength (λ) on 50-m MOCVD YBCO CC tape produced by SuperPower, Inc. Spectra (a) and (b) were recorded at two positions 2 mm apart using 8- μm laser spot size (SS) and λ of 633 nm. Spectrum (c) was recorded at position proximal to those of (a) and (b) using SS of 60- μm and λ of 785 nm.

(4) The creation of a database of standard Raman spectra for various forms of YBCO (e.g., orthorhombic, tetragonal, cation disordered, oxygen disordered, etc.) and common second phases, such as barium cuprates, $\text{Y}_2\text{Cu}_2\text{O}_5$ ("202"), Y_2BaCuO_5 ("211"), and CuO , is centrally important to sorting out the compositions revealed by Raman spectroscopy. An example of this aspect of using Raman spectroscopy as a coated conductor characterization tool is shown in Fig. 10, where we have twice plotted (in solid line) the Raman spectrum obtained at a particular location in a low- I_c region of the 50-m SuperPower tape. In one case we have overlaid (in dotted line) the spectrum of our BaCuO_2 standard and in the other case we have overlaid (in dotted line) the standard spectrum of "211". (The YBCO phonons are indicated with yellow shading.) Clearly, there is a match to the BaCuO_2 spectrum but not to the "211" spectrum. We have found in this work that the best way to prepare impurity phase standards is to press well-characterized impurity phase powder into a pellet at ambient temperature, using KBr as a binder. This tends to consolidate the respective impurity phase into a textured host medium similar to that represented by the YBCO film.

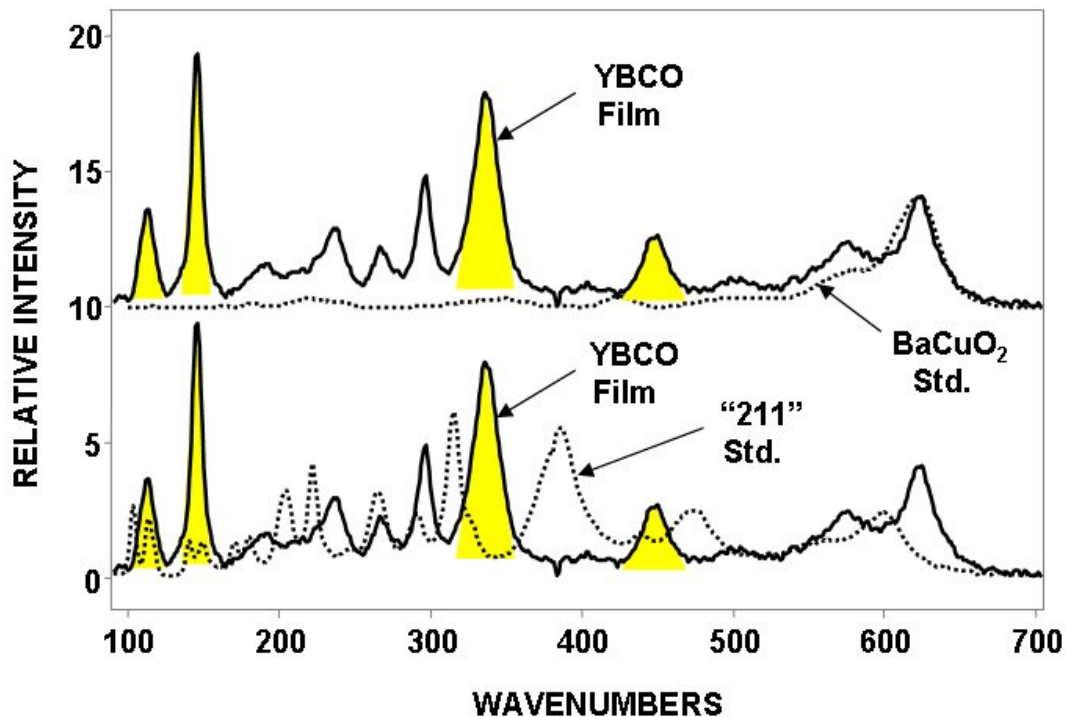


Fig. 10. Raman spectrum (shown twice by solid line) taken in low- I_c region of 50-m MOCVD YBCO CC tape produced by

SuperPower, Inc. Spectra of BaCuO₂ and "211" standards (dotted lines) are overlaid for comparison. Shaded bands are YBCO phonons.

References

1. Argonne National Laboratory, Practical Superconductor Development for Electrical Power Application, Quarterly Report for Jan.-Mar., 2003.
2. Argonne National Laboratory Practical Superconductor Development for Electrical Power Application, Quarterly Report for Jan. Mar., 2004.
3. K. Venkataraman, D.F. Lee, K. Leonard, L. Heatherly, S. Cook, M. Paranthaman, M. Mika, and V.A. Maroni, Superconductor Science and Technology 17, 739-749 (2004).

Interactions

Balu Balachandran reviewed the Korean HTSC program during April 20-21 in Gyeonju, South Korea.

J. P. Singh and Shankar Srinivasan attended the American Ceramic Society Annual Meeting during April 19-21, 2004 in Indianapolis and presented a talk on the mechanical properties of 2G films.

Balu Balachandran attended the FWP review meeting in DOE/HQ, Washington DC, on May 25, 2004.

Balu Balachandran attended the CCAS meeting in Washington DC on May 26, 2004.

Beihai Ma gave a talk on HTSC at the University of Chicago Review of Energy Technology programs on June 17, 2004 at ANL.

Rabi Bhattacharya (UES) visited ANL on May 6, 2004.

Y. S. Cha attended the Technical Advisory Board meeting for the IGC-SuperPower MFCL project in Schenectady, New York on May 4, 2004.

Vic Maroni attended a Wire Development Group meeting June 2-3, 2004 in Madison, WI. June 2 was devoted to 1G wire development, and involved participants from AMSC, ANL, UWM, and LANL; June 3 was devoted to 2G wire development and involved AMSC, ANL, UWM, LANL, and ORNL.

Publications and Presentations

Published/Submitted

R. M. Baurceanu, S. E. Dorris, T. Wiencek, B. Ma, R. E. Koritala, V. A. Maroni, K. Venkataraman, M. Mika, and U. Balachandran, Optimum Copper Content of Silver for $\text{YBa}_2\text{Cu}_3\text{O}_{7-\delta}$ (YBCO) Coated Conductors, *Physica C*, 406, 169-175 (2004).

K. K. Uprety, B. Ma, R. E. Koritala, R. M. Baurceanu, T. P. Weber, B. L. Fisher, S. E. Dorris, R. A. Erck, V. A. Maroni, and U. Balachandran, Growth of YBCO Film on SrRuO_3 -buffered MgO Substrate, *Superconductor Science and Technology*, 17, 671-675 (2004).

T. P. Weber, B. Ma, U. Balachandran, and M. McNallan, Fabrication of Biaxially-Textured Magnesium Oxide Thin Films by Ion-Beam-Assisted Deposition, Submitted to *Thin Solid Films* (March 2004).

U. Balachandran, Trends and Prospects of the Superconducting Wire, Invited Publication to Efficiency, Speed, Environment-friendly (ESE), published by the Center for Applied Superconductor Technology (CAST), South Korea, No. 03, 30-33 (2004).

P. S. Shankar, S. H. Majumdar, S. Majumdar, and J. P. Singh, Finite Element Modeling of Residual Stresses in Multilayered Coated Conductors, Paper presented at the 106th Ann. Mtg. of the American Ceramic Society, Indianapolis, April 18-21, 2004.

Patents: 2000-2003

Fabrication of High Temperature Superconductors

Uthamalingam Balachandran, Stephen E. Dorris, Beihai Ma, and Meiya Li
U.S. Patent No. 6,579,360 (June 17, 2003).

Metallic Substrates for High-Temperature Superconductors

T. Truchan, D. Miller, K. C. Goretta, U. Balachandran, and R. Foley (U. of IL)
U.S. Patent No. 6,455,166 (Sept. 24, 2002).

Method for Preparing High-Temperature Superconductor
Uthamalingam Balachandran and Michael P. Chudzik
U.S. Patent No. 6,361,598 (March 26, 2002).

Shielded High- T_c BSCCO Tapes or Wires for High-Field Applications
Uthamalingam Balachandran, Milan Lelovic, and Nicholas G. Eror
U.S. Patent No. 6,252,096 (June 26, 2001); U.S. Patent 6,466,805 (Oct. 15, 2002).

Thermomechanical Means to Improve Critical Current Density of BSCCO Tapes
Uthamalingam Balachandran, Roger B. Poeppel, Pradeep Haldar (IGC), and
Lesizek Motowidlo (IGC), U.S. Patent 6,240,619 (June 5, 2001).

Method of Manufacturing a High-Temperature Superconductor with Improved
Transport Properties
Uthamalingam Balachandran, Richard Siegel, and Thomas Askew
U.S. Patent No. 6,191,075 (February 20, 2001).

Bearing Design for Flywheel Energy Storage Using High- T_c Superconductors
John R. Hull and Thomas M. Mulcahy
U.S. Patent No. 6,153,958 (Nov. 28, 2000).

Method and Apparatus for Measuring Gravitational Acceleration Utilizing a
High- Temperature Superconducting Bearing
John R. Hull
U.S. Patent 6,079,267 (June 27, 2000).

Improvements in Levitation Pressure and Friction Losses in Superconducting
Bearings,
John R. Hull
U.S. Patent 6,175,175 (January 16, 2001).

Trapped Field Internal Dipole Superconducting Motor/Generator
John R. Hull
U.S. Patent 6,169,352 (January 2, 2001).

Reluctance Apparatus for Flywheel Energy Storage
John R. Hull
U.S. Patent 6,097,118 (August 1, 2000).

Large Area Bulk Superconductors
Dean J. Miller and Michael B. Field
U.S. Patent 6,410,487 (June 25, 2002).

Figure Captions

- Fig. 1: The tilt angle β as a function of α for YBCO (005) plane on YBCO/SRO/ISD-MgO substrate.
- Fig. 2: Transport J_c [solid circle] and x-ray ϕ -scan FWHM values for YBCO (005) peak [open circle] as a function of substrate inclination angle α .
- Fig. 3: Inductive T_c [solid square] and superconducting transition temperature width ΔT [open square] as a function of α for YBCO films grown on SRO buffered ISD-MgO substrate.
- Fig. 4: Plot of normalized I_c ($I_c/I_{c(MAX)}$) versus position along the length of a 12 meter MOCVD YBCO CC tape produced by SuperPower, Inc. The sketch below the graph identifies the segment of the tape interrogated by Raman microscopy and shows the general location of the scan paths tracked during the Raman survey.
- Fig. 5: Raman spectra recorded at selected locations between the 100 cm and 1000 cm marks in Fig. 1. The numbers along the right side of the plot correspond to the position in centimeters along the horizontal axis of the graph in Fig. 1.
- Fig. 6: (a) Intensity relief graphic constructed from the series of closely spaced Raman scans recorded between the 500 cm and 515 cm positions in Fig. 1. (All the phonon intensities are normalized to the intensity of the YBCO O₂⁺/O₃⁻ mode at ca. 320 cm⁻¹.) (b) Graph showing normalized I_c at four positions between 500 cm and 515 cm.
- Fig. 7: Schematic diagram of the Raman probe concept devised for on-line monitoring of moving CC tape after YBCO deposition.
- Fig. 8: Raman spectra recorded as a function of laser spot size (SS) at two arbitrarily chosen positions on a 50 meter MOCVD YBCO CC tape produced by SuperPower, Inc. Spectra (a) and (b) were from a low I_c region; spectra (c) and (d) were from a high I_c region.
- Fig. 9: Raman spectra recorded as a function of proximal location and laser wavelength on a 50 meter MOCVD YBCO CC tape produced by SuperPower, Inc. Spectra (a) and (b) were recorded at two positions 2 mm apart using an 8 μ m laser spot size (SS) and a 633 nm excitation wavelength (λ). Spectrum (c) was recorded at a position proximal to that

of (a) and (b) using a 60 μm laser spot size and a 785 nm excitation wavelength.

Fig. 10. Raman spectrum (solid line—shown twice) taken in a low I_c region of the 50 meter MOCVD YBCO CC tape produced by SuperPower, Inc. Spectra of BaCuO_2 and “211” standards (dotted lines) are overlaid for comparison. The shaded bands are YBCO phonons.